Characterization of chicken muscle disorders through metabolomics, pathway analysis, and water relaxometry: a pilot study

Nara R. B. Cônsolo,*[,1] Linda M. Samuelsson,[†] Luís C. G. S. Barbosa,[‡] Tatiana Monaretto,[§] Tiago B. Moraes,[#] Vicente L. M. Buarque,* Angel R. Higuera-Padilla,[‖] Luiz A. Colnago,[‖] Saulo L. Silva,* Marlon M. Reis,[†] André C. Fonseca,[‡] Cristiane S. da S. Araújo,[‡] Bruna G. de S. Leite,* Fabricia A. Roque,* and Lúcio F. Araújo*[,2]

*Faculty of Animal Science and Food Engineering, University of São Paulo, Pirassununga 13635-900, SP, Brazil; [†]AgResearch, Grasslands Research Centre, Palmerston North 4442, New Zealand; [‡]School of Veterinary Medicine and Animal Sciences, University of São Paulo, Pirassununga 13635-900, SP, Brazil; [§]São Carlos Institute of Chemistry, University of São Paulo, São Carlos 13566-590, SP, Brazil; [#]Department of Chemistry, Institute of Exact Sciences, Federal University of Minas Gerais, Belo Horizonte 31270-901, MG, Brazil; and [‖]EMBRAPA Instrumentação, São Carlos 13560-970, SP, Brazil

ABSTRACT Metabolite profiles of chicken breast extracts and water mobility in breasts were studied using proton nuclear magnetic resonance (**^{1}H-NMR**) spectroscopy and time-domain NMR (**TD-NMR**) relaxometry, respectively, using normal breast (**NB**), and wooden breast (**WB**) and white striping (**WS**) myopathies in broilers. One thousand eight hundred sixty broilers were raised to commercial standards, receiving the same diets that were formulated as per the different growth stages. At 49 D of age, 200 animals were slaughtered following routine commercial procedures, and at 4 h postmortem, the whole breast (pectoralis major muscle) was removed and visually inspected by an experienced meat inspector who selected NB (without myopathies) and samples with the presence of WS and WB myopathies. Fifteen breasts (5 each of NB, WS, and WB) were analyzed through TD-NMR relaxometry, and samples of approximately 20 g were taken from each breast and frozen at −80°C for metabolite profiling through ^{1}H-NMR spectroscopy. Multivariate statistical analysis was used to evaluate the effect on water relaxometry and metabolite profile in accordance with the presence and type of myopathy in the breast. ^{1}H-NMR data showed that the metabolite profiles in WS and WB breasts were different from each other and from NB. This pilot study shows that myopathies appear to be related to hypoxia, connective tissue deposition, lower mitochondrial function, and greater oxidative stress compared with NB. The longitudinal and transverse relaxation time of the breasts determined by TD-NMR relaxometry was shorter for NB than that for WS and WB, indicating greater water mobility in breasts affected by myopathies. ^{1}H-NMR spectroscopy can be used to differentiate the metabolism of WS, WB, and NB, and TD-NMR has the potential to be a fast, simple, and noninvasive method to distinguish NB from WB and WS. As a practical application, the metabolomic profile as per the occurrence of breast myopathies may be used for a better understanding of these issues, which opens a gap to mitigate the incidence and severity of WS and WB. In addition, the present study brings an opportunity for the development of a new and objective tool to classify the incidence of breast myopathies through TD-NMR relaxometry.

Key words: chicken breast myopathy, metabolomics, NMR spectroscopy, TD-NMR relaxometry, water mobilization

2020 Poultry Science 99:6247–6257
https://doi.org/10.1016/j.psj.2020.06.066

INTRODUCTION

Brazil is the world's second largest producer, and the largest exporter, of poultry meat; however, the poultry industry is facing emergent cases of myopathies in modern commercial broilers, affecting the pectoralis major muscle (Sihvo et al., 2013). The poultry industry has been

Received February 7, 2020.
Accepted June 29, 2020.

[1]Present address: AgResearch, Grasslands Research Centre, Tennent Drive, 11 Dairy Farm Rd, Palmerston North 4442, New Zealand.
[2]Corresponding author: lfaraujo@usp.br

focusing on the improvement of carcass quality with higher breast yield and muscle mass development and less abdominal fat (López et al., 2011).

According to Havenstein (2006), the 85 to 90% improvement in bird growth rate observed over the last 5 decades was achieved by genetic selection, whereas the remaining 10 to 15% of the observed change in this characteristic was due to improved nutritional plans. However, this intensive selection for fast early growth rate has led to the development of some muscle abnormalities and metabolic disorders in modern broiler breeds. In addition, a strong genetic determinant of the myopathy condition was recently found in fast-growing chickens (Alnahhas et al., 2016).

White striping (**WS**) and wooden breast (**WB**) are 2 phenomena affecting meat quality, occurring in 50% of chicken breasts under commercial broiler growth conditions (Petracci et al., 2013; Trocino et al., 2015). Both myopathies have a similar histologic impact on the muscle, characterized by the presence of myodegeneration and variable amounts of interstitial connective tissue accumulation, leading to muscle degeneration (Sihvo et al., 2013). White striping often affects the breast muscle and exhibits a fatty appearance, marbled with white striations running parallel to the muscle fibers (Kuttappan et al., 2012; Trocino et al., 2015). Wooden breast is characterized by remarkable diffuse or focal palpatory hardness throughout the breast area and often exhibits a pale color, viscous fluid, and hemorrhagic lesions (Sihvo et al., 2013).

Affected breast fillets are rejected by consumers, resulting in significant economic losses to the poultry industry (Kuttappan et al., 2012). The occurrence of myopathies in broiler breasts is generally linked to rapid increases in muscle growth rates, approaching maximum physiologically sustainable rates; however, the etiology of WS and WB is not fully understood. To this end, metabolomics may be used for better understanding of the underlying metabolism and consequently lead to mitigation strategies for the occurrence of these myopathies. Recently, Mutryn et al. (2015) reported that WB causes increased oxidative stress, localized hypoxia, higher levels of intracellular calcium, and switching of the fiber muscle type compared with breasts without myopathies. Boerboom et al. (2018) found that hypoxia was the most likely cause or initiator of WS in broilers. Other authors have explained that WS and WB are 2 degenerative myopathies resulting in breasts with a higher fat and lower protein content, elevated ultimate pH, increased moisture, and poorer water-holding capacity (Mudalal et al., 2014, 2015; Wold et al., 2017, 2019; Baldi et al., 2020). However, to date, no study has been conducted to compare WB with WS and to look at the metabolic pathways affected by these myopathies.

In addition, the use of time-domain nuclear magnetic resonance (**TD-NMR**) relaxometry has been reported as a fast and objective way to discriminate broiler breast myopathies from normal breast (**NB**) (Tasoniero et al., 2017; Xing et al., 2017). Recently, Tasoniero et al. (2017) analyzed WB samples, but not WS samples, with TD-NMR relaxometry using the Carr–Purcell–Meiboom–Gill (**CPMG**) pulse sequence and observed that the extramyofibrillar water population and the T_{21} value increased in WB samples when compared with normal samples. Xing et al. (2017) also used TD-NMR relaxometry to study the functional properties of NB and WB, and they observed that raw WB had a higher proportion of extramyofibrillar water and greater mobility of intramyofibrillar water than NB.

We hypothesize that metabolite profiles can differentiate NB from those affected by myopathies and that the profiles of WB and WS are also different. In addition, we hypothesize that water mobility changes in response to the myopathies and that this may allow TD-NMR to be used as a tool for fast identification of the presence of WS or WB. The aim of this research was to investigate the metabolite profiles of breast tissue affected by WB and WS myopathies in broilers using a proton nuclear magnetic resonance (**^{1}H-NMR**)–based metabolomic approach and to identify the most relevant metabolic pathways linked to the development of myopathies. In addition, TD-NMR relaxometry analysis using transverse ($\mathbf{T_2}$) and longitudinal ($\mathbf{T_1}$) signals was performed to better understand these myopathies through water mobility. To our knowledge, no previous study has combined ^{1}H-NMR metabolomics and TD-NMR relaxometry to better understand the WB and WS myopathies in the breast from chicken broilers.

MATERIALS AND METHODS

The animal procedures in this study were conducted in accordance with the Institutional Animal Care and Use Committee Guidelines of the University of São Paulo and were approved by the School of Veterinary Medicine and Animal Science Animal Ethics Committee (Protocol Number: 1713280918).

Sample Collection

One thousand eight hundred sixty broilers were raised to commercial standards; the temperature was controlled in 45 × 10 m b, with negative pressure ventilation, and cool cells with insulated asbestos roofing. The animals were allocated in pens measuring 1.0 × 1.2 m, and each pen was provided with nipple drinkers, 1 tube feeder, and rice husk litter. Feed and water were provided ad libitum for all of the broiler chickens during the whole experimental period. The barn was heated using an automatic gas heating system that was activated depending on the internal temperature. The room temperature was set at 32°C in the first week, and then, it was gradually decreased as per the housing recommendations for the breed. The illumination schedule was set in accordance with the Cobb broiler management guide. The broilers received the same diets, which were formulated as per the different growth stages: prestarter (1–7 D), starter (8–21 D), grower (22–33 D), finisher (34–42 D), and withdrawal (43–49 D).

At 49 D of age, 200 animals were slaughtered following routine commercial procedures consisting of hanging, electrical stunning, bleeding, scalding, defeathering, evisceration, chilling, and cooling. At 4 h postmortem, the whole breast (pectoralis major muscle) was removed and visually inspected by an experienced meat inspector, who selected NB (without myopathies, n = 5) and samples with the severe presence of WS (n = 5) and WB (n = 5) myopathies, as per the criteria established by Kuttappan et al. (2012) and Sihvo et al. (2013).

The breasts were placed in Ziploc bags and transported on ice to the Nuclear Magnetic Resonance Laboratory (EMBRAPA, São Carlos) for analyses using TD-NMR relaxometry, where the whole breast was used. For ^{1}H-NMR spectroscopy, samples of approximately 20 g were taken from each breast and frozen at −80°C until analysis. The samples were trimmed from the superficial (an inch deep) and cranial part of the breast, where the myopathies were detected.

Extraction of Polar Metabolites From Breast

Frozen breast (0.5 g) was macerated and homogenized using a blender (Ultra-Turrax, T 25 digital; IKA, Campinas, SP, Brazil), and metabolites were extracted with 3.5 mL of a solution of cold methanol and water solution (4:3 v/v) while vortexing for 1 min, as previously described by Beckonert et al. (2007). Samples were left on ice for 15 min and were then centrifuged for 15 min at 10,000 × *g* at 4°C to remove precipitated protein and connective tissue. Supernatants were carefully transferred to Eppendorf tubes and vacuum-dried (Itasul Import and Instrumental Technical Ltda, Porto Alegre, RS, Brazil). The residue was reconstituted in 600 μL of 100 mmol/L phosphate buffer (containing 10% D_2O and 90% H_2O, pH 7.0) and 60 μL internal standard solution (containing 5 mmol/L 3-(trimethylsilyl)-1-propanesulfonic acid sodium salt [**DSS**] as a quantitation standard and chemical shift reference and 100 mmol/L imidazole as a pH indicator) was added. Samples were centrifuged at 10,000 × *g* for 3 min at 4°C to remove any precipitate; 600 μL of the supernatant was transferred to standard 5 × 178 mm thin-walled NMR tubes (VWR International).

NMR Spectroscopy

One-dimensional (**1D**) ^{1}H-NMR was used for metabolite profiling, and the analyses were performed at EMBRAPA Instrumentation (São Carlos, São Paulo state). Proton NMR spectra were acquired at 300 K on a Bruker Avance 14.1 T spectrometer (Bruker Corporation, Karlsruhe, Baden-Württemberg, Germany) at 600.13 MHz for ^{1}H, using a BBO 5-mm probe. D_2O was used as a lock solvent and DSS as the chemical shift reference for ^{1}H. Standard 1D proton NMR spectra were acquired using a single 90° pulse experiment, and each spectrum was the sum of 64 free induction decays. Water suppression was performed using the Bruker "zgesgp" pulse sequence (excitation sculpting with gradients), and the following acquisition parameters were used: 13.05 μs 90° pulse, 0.5 s relaxation delay, 64k data points, 64 scans, 3.89 s acquisition time, and 14.03 ppm spectral width.

Spectral Processing and Metabolite Quantitation

Proton NMR spectra were processed using Chenomx NMR Suite Professional 7.7 software (Chenomx Inc., Edmonton, Canada): phasing and baseline correction were performed, and the pH was calibrated using the resonances from imidazole. The spectra were referenced to the DSS methyl peak at 0.00 ppm. The same peak was also used as a chemical shape indicator, that is as an internal standard for quantitation.

Metabolites were quantified in the 1D ^{1}H-NMR spectra of breast extracts using the Profiler module of Chenomx NMR Suite Professional software with an inbuilt 1D spectral library. Quantitation was based on comparing the area of selected metabolite peaks with the area under the DSS methyl peak, which corresponded to a known concentration of 0.5 mmol/L in all samples. The resulting metabolite concentration table (56 metabolites × 15 samples) was exported to Excel where sample identifiers were added.

TD-NMR Relaxometry

Whole breasts were analyzed by TD-NMR using the CPMG pulse sequence pulse (De Andrade et al., 2011) and continuous wave free precession with a low flip angle, also known as the CWFP-T_1 pulse sequence (Moraes et al., 2019). The TD-NMR analyses were performed in an SLK-IF-1399 (0.23 T or 9 MHz for ^{1}H resonance frequency) spectrometer (Spinlock, Córdoba, Argentina) using a 10-cm probe at 23°C. The CPMG sequence was performed using a 90° pulse followed by a train of 180° pulses of 17 and 34 μs, respectively, and echo times of 0.3 ms with a total of 1,500 echoes. The CWFP-T_1 sequence was performed using a 180° pulse followed by a train of 10° pulses of 6.28 μs, an interpulse delay of 0.3 ms and 1,501 CWFP-T_1 data points. In both sequences, the signals were averaged with 4 scans.

Data Analysis

The metabolomic data were analyzed using MetaboAnalyst 4.0 (http://www.metaboanalyst.ca/). The metabolite concentration table was uploaded to MetaboAnalyst, and the data were log transformed and Pareto scaled before analysis. Supervised (partial least squares-discriminant analysis) data analysis was performed. Cross validation was performed for partial least squares-discriminant analysis using the method leave-one-out cross-validation and the performance measure "accuracy." The variable importance in the projection (**VIP**) plot was used to rank the metabolites based on their importance in discriminating the groups. Metabolites with the highest VIP values are the most powerful group discriminators.

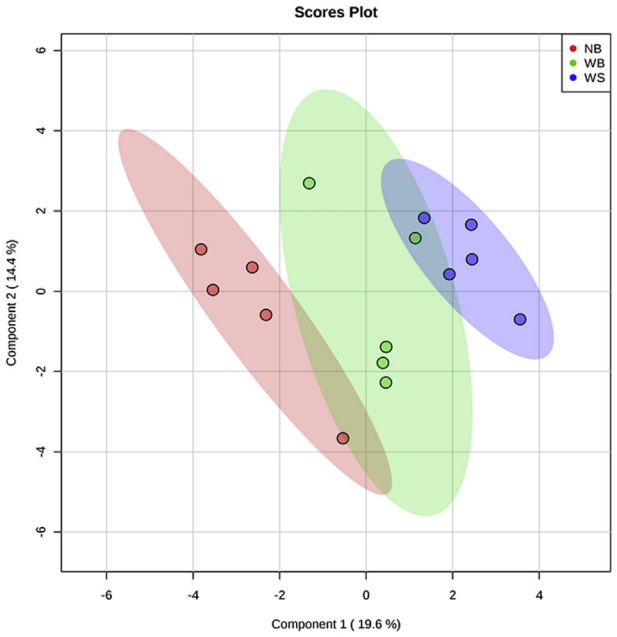

Figure 1. PLS-DA scores plot of metabolite profiles in chicken breasts. Abbreviations: NB, normal breast; PLS-DA, partial least squares-discriminant analysis; WB, wooden breast; WS, white stripping.

Metabolites with VIP values >1 were considered significant and metabolites with VIP values >2 were highly significant. Pathway analyses were conducted using metabolite data sets for each group, using the *Gallus gallus* library in MetaboAnalyst, and based on the exploratory nature of this study, we included pathways with a raw P of <0.1 as being of high pathway impact and interest.

The T_1 and T_2 values, obtained with CPMG and CWFP-T_1 in TD-NMR relaxometry, were calculated using in-house inverse Laplace transform (**ILT**) software based on the Butler–Reeds–Dawson method (Venkataramanan et al., 2002). The TD-NMR relaxation data were analyzed with multivariate methods using R software and MetaboAnalyst 4.0. The TD-NMR data were normalized and mean centered, and unsupervised (PCA) analyses were performed.

RESULTS

Fifty-six metabolites were quantified in the ^{1}H-NMR spectra, including nonessential amino acids, essential amino acids, small peptides, amino acid derivatives, organic acids, nucleic acids, sugar, vitamins, and cellular antioxidants (descriptive statistics; Supplementary Table 1). Lactate was the most abundant metabolite in all 3 types of breast, followed by creatine and carnosine.

Partial least squares-discriminant analysis was used to visualize the differences in metabolite profiles between the 3 groups (Figure 1). Although the first 2 principal components only explain 34% of the variance in the data, the model is still valid, as per the cross-validation test results (R^2 = 0.92 and Q2 = 0.53). The scores plot (Figure 1) shows a separation between the control (NB) and WS groups, indicating that their metabolite profiles are different. However, the WB group overlaps with both the NB and WS groups, suggesting that the metabolite profile of WB shares similarities with those of both NB and WB, although in different ways.

Metabolite Profiles: WB vs. WS, NB vs. WB, and NB vs. WS

After establishing that the metabolite profiles of the 3 groups (NB, WS, and WB) seem to be different (Figure 1), pairwise comparisons using partial least squares-discriminant analysis were conducted to elucidate the specific differences between groups. The top 15 metabolites discriminating WB from WS, NB from WS, and NB from WB are shown in Figures 2A–2C. A higher VIP value is correlated with a greater contribution of the corresponding metabolite to discrimination of the 2 groups. Butyrate was the most important metabolite for discriminating between WS and WB, with the butyrate concentration in WB double that in WS. Glutamate, pyruvate, 3-methylhistidine, and leucine were also important for the discrimination of these 2 types of myopathy. Several of the metabolites important for differentiating NB from WS were also important for differentiating NB from WB, but there were also some important differences (Figures 2B, 2C). Malonate, taurine, threonine, and arginine were the most important metabolites for differentiating NB from WS, whereas niacinamide, choline, arginine, malonate, and inosine monophosphate (**IMP**) were the most important metabolites for differentiating NB from WB (Figures 2B, 2C).

Pathway Analysis

The most relevant pathways differentiating WS from WB were cysteine and methionine metabolism, glutathione metabolism, taurine and hypotaurine metabolism, glycine, serine and threonine metabolism, glutamine and glutamate metabolism, and phenylalanine, tyrosine, and tryptophan biosynthesis (Figure 3A). When comparing NB with either of the 2 myopathies (WS or WB), the following pathways were affected the most: nicotinate and nicotinamide metabolism, glycine, serine, and threonine metabolism, arginine and proline metabolism, and β-alanine metabolism (Figures 3B, 3C). However, taurine and hypotaurine metabolism and aminoacyl-tRNA biosynthesis were only affected when comparing NB with WS. Glycerophospholipid metabolism and alanine, aspartate, and glutamate metabolism were only affected when comparing NB with WB. All the important metabolites colored in red in the pathway analysis (Figures 3A–3C) are collated in Table 1 along with their respective pathways and their impacts on these pathways. The highlighted pathways are better described in Supplementary Figure 1.

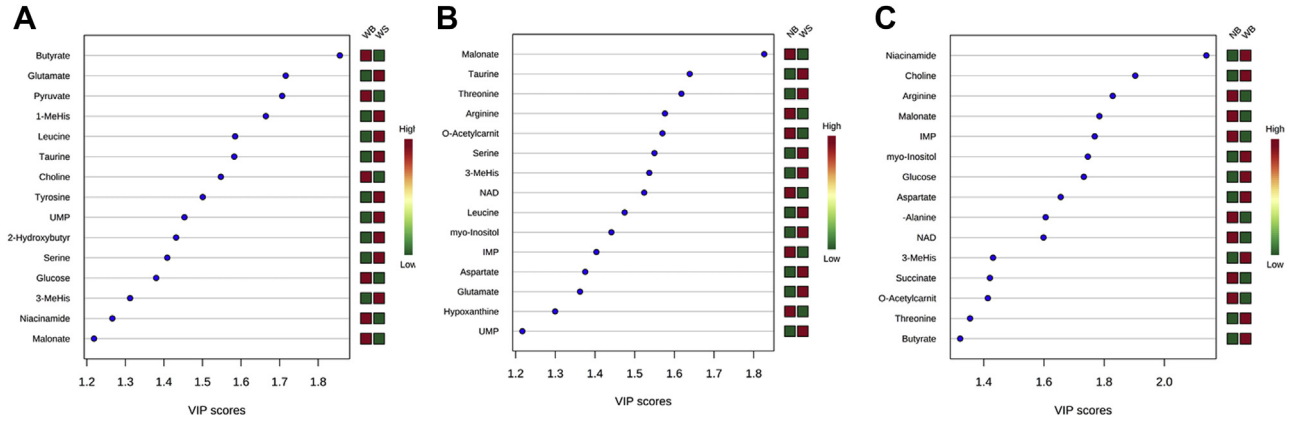

Figure 2. Variable importance in projection (VIP) plots from pairwise PLS-DA analyses of groups: (A) WS vs. WB ($R^2 = 0.99$ and Q2 = 0.55); (B) NB vs. WS ($R^2 = 0.99$ and Q2 = 0.60); (C) NB vs. WB ($R^2 = 0.99$ and Q2 = 0.57). Abbreviations: NB, normal breast; PLS-DA, partial least squares-discriminant analysis; WB, wooden breast; WS, white stripping.

TD-NMR Relaxometry

Supplementary Figures 2A, 2B show the T_2 and T_1 relaxation exponential signals obtained with a wide-bore TD-NMR spectrometer (Pereira et al., 2013) using the CPMG and CWFP-T_1 pulse sequences, respectively. Both relaxation curves show that NB samples had shorter relaxation times (shorter exponential curves) than WS and WB samples (Figure 4A). The T_1 and T_2 values were calculated by the ILT of the CWFP-T_1 and CPMG signals. The ILT relaxation distribution spectra show 2 T_1 values at approximately 100 (T_{11}) and 450 (T_{12}) ms, and 3 T_2 values at approximately 2 (T_{2B}), 50 (T_{21}), and 110 (T_{22}) ms. The area of the strongest peaks T_{12} and T_{21} in the ILT relaxation spectra represent more than 85% of the total area, and therefore, only these 2 signals were used in the subsequent data analyses.

Figure 4A shows the average and SD of the T_{12} and T_{21} values of NB, WS, and WB samples. Both T_{12} and T_{21} were lower in NB samples (450 and 45 ms, respectively) and higher in both WB (470 and 50 ms, respectively) and WS (490 and 50 ms, respectively). The error bars show a larger dispersion of relaxation times for WS samples. Figures 4B, 4C show the PCA scores plots for CPMG (a) and CWFP-T_1 (b) data. Both scores plots show that the NB and WB groups are separated from each other, whereas the WS group overlaps with both due to greater variation in the WS relaxation data.

DISCUSSION

Detection of WS and WB is generally conducted on the deboning line in a chicken processing plant during routine inspection of carcasses. Trained staff classify the occurrence and severity of myopathies through visual examination, manual palpation, or both of the pectoralis major muscle (Kuttappan et al., 2012, 2013). Research to date points to a complex etiology and a polygenic inheritance of these broiler breast defects (Mutryn et al., 2015; Zambonelli et al., 2016; Papah et al., 2018). Indeed, gene expression studies show that several genes are differentially expressed in the pectoralis major affected by WS, WB, or both, compared with unaffected (or only mildly affected) cases (Petracci et al., 2019). Nevertheless, WS and WB abnormalities exhibit distinctive phenotypes that may be considered as individual responses to the profound alterations in muscle tissue induced by genetic selection. However, to date, no studies have successfully identified biomarkers that will be able to distinguish WS from WB.

In this context, the application of metabolomic analyses in breasts affected by myopathies may be helpful for obtaining a better comprehension of the pathophysiology of these defects (Petracci et al., 2019). Some studies have highlighted certain metabolites as potential biomarkers for the underlying etiology of either WS or WB in comparison with NB (Boerboom et al., 2018; Abasht et al., 2019), whereas the present study includes comparison of the metabolomics signature between pectoralis major muscles affected by WS and WB in modern broiler chickens and the most relevant pathways correlated with the differentiation of these 2 myopathies. It is important to emphasize that the present study was a preliminary investigation about metabolite variation in accordance with = WS and WB occurrence in broilers. The major limitation of this pilot study was the number of samples; however, it will provide the groundwork for further studies investigating metabolites that are differently expressed between the pectoralis major affected by WS, WB, or both and unaffected cases. Further studies would preferably include more extensive metabolite coverage: the extraction method and analytical technique used in this study limited the coverage to polar metabolites with a concentration of >0.01 mmol/L.

Major structural and biochemical changes take place during the conversion of muscle to meat. In poultry, this process is completed within 1 to 2 h (Dransfield and Sosnicki, 1999). Hence, the metabolite profiles of breasts sampled 4 h postmortem are different from those in the live bird. However, several studies have confirmed clear linkages between preslaughter conditions and metabolism and subsequent meat composition and biochemistry (Savenije et al., 2002; Carrillo et al., 2016;

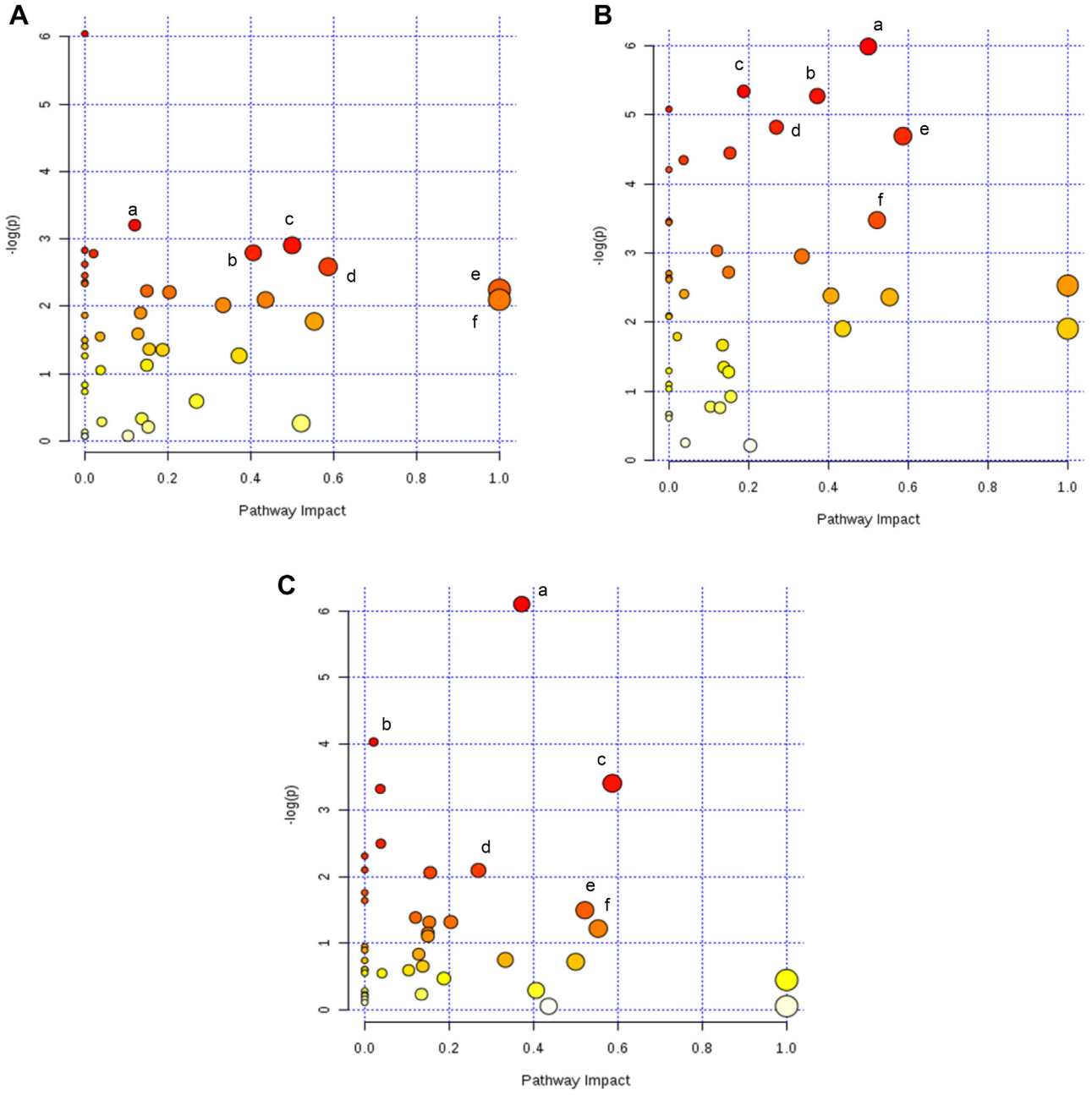

Figure 3. Pathway analysis using all metabolites that were significantly different between the groups: (A) WS vs. WB (a) cysteine and methionine metabolism, (b) glutathione metabolism, (c) taurine and hypotaurine metabolism, (d) glycine, serine, and threonine metabolism, (e) glutamine and glutamate metabolism, (f) phenylalanine, tyrosine, and tryptophan biosynthesis; (B) NB vs. WS (a) taurine and hypotaurine metabolism, (b) nicotinate and nicotinamide metabolism, (c) aminoacyl-tRNA biosynthesis, (d) arginine and proline metabolism, (e) glycine, serine, and threonine metabolism, (f) β-alanine metabolism; (C) NB vs. WB (a) nicotinate and nicotinamide metabolism, (b) glycerophospholipid metabolism, (c) glycine, serine, and threonine metabolism, (d) arginine and proline metabolism, (e) β-alanine metabolism, (f) alanine, aspartate, and glutamate metabolism. The x-axis displays pathway impact values from the pathway topology analysis, and the y-axis the *P*-values from the pathway enrichment analysis. The darker the color, the more significant the pathway. Abbreviations: NB, normal breast; WB, wooden breast; WS, white stripping.

Zawadzki et al., 2017; Soglia et al., 2019b; Cônsolo et al., 2020; Xing et al., 2020), which allows postmortem metabolite data to be linked back to biochemical pathways in the live animal, at least to some extent.

Through metabolite concentrations (Supplementary Table 1 and Figure 2A) and metabolic pathway analysis (Figure 3A), data from the present study indicate that the differences between WS and WB are 1) different stages of muscle hypoxia and 2) higher collagen deposition in breasts affected by WB. The lower amounts of malonate in WS than those in the WB group (Figure 2A) could indicate more binding of malonate with succinate dehydrogenase enzyme in WS muscle. This enzyme is responsible for the synthesis of fumarate from succinate in the Krebs cycle (Kim, 2002). Its lower amount observed in WS may be due to its complexation with SD. Malonate can block the active site of this enzyme, thus competing with succinate, which can result in decreased cellular respiration and increased muscle hypoxia. This is supported by other recent findings

Table 1. Main pathways associated with differentiation between NB, WS, and WB breasts and their most important metabolites.[1]

Pathways	Important metabolites (red in the map)	Raw *P*	-Log(*p*)	FDR	Impact
WS vs. WB					
Cysteine and methionine metabolism	Pyruvate	0.04057	3.204	0.314	0.120
Glutathione metabolism	Glutamate	0.06117	2.794	0.314	0.406
Taurine and hypotaurine metabolism	Taurine	0.05476	2.904	0.316	0.500
Glycine, serine and threonine metabolism	Choline and pyruvate	0.07524	2.587	0.314	0.580
Glutamine and glutamate metabolism	Glutamate	0.10587	2.245	0.314	1
Phenylalanine, tyrosine and tryptophan biosynthesis	Tyrosine	0.12283	2.096	0.314	1
NB vs. WS					
Taurine and hypotaurine metabolism	Taurine	0.00250	5.990	0.050	0.500
Nicotinate and nicotinamide metabolism	NAD+	0.00579	5.151	0.050	0.372
Aminoacyl-tRNA biosynthesis	Arginine, serine and threonine	0.00462	5.376	0.050	0.187
Arginine and proline metabolism	Arginine and glutamate	0.00482	5.334	0.050	0.269
Glycine, serine and threonine metabolism	Threonine	0.05154	2.965	0.129	0.586
β-Alanine metabolism	Aspartate and β-Alanine	0.02813	3.570	0.116	0.521
Glutamine and glutamate metabolism	Glutamate	0.04457	3.110	0.129	1
NB vs. WB					
Nicotinate and nicotinamide metabolism	Niacinamide	0.00223	6.103	0.091	0.372
Glycerophospholipid metabolism	Choline	0.01781	4.027	0.365	0.020
Glycine, serine and threonine metabolism	Threonine and choline	0.03318	3.405	0.370	0.586
Arginine and proline metabolism	Arginine and aspartate	0.12315	2.094	0.579	0.269
Alanine, aspartate and glutamate metabolism	Aspartate	0.29566	1.218	0.754	0.553
β-Alanine metabolism	Aspartate	0.22422	1.495	0.733	0.521
Glutamine and glutamate metabolism	Glutamate	0.09918	2.310	0.822	1

[1]Important metabolites are those represented in red box in the pathway analysis (Figures 3A–3C) as per its ID in KEGG pathway (accessible at http://www.genome.jp/kegg/pathway.html).

reporting that breasts affected by WS myopathies are characterized by a severe hypoxic status (Mutryn et al., 2015; Boerboom et al., 2018; Abasht et al., 2019). In addition, Boerboom et al. (2018) noted that hypoxia could be considered a triggering event for WS alterations in broiler chickens.

It is important to emphasize that this result did not represent the absence of hypoxia in WB fillets, as there is some evidence that WB appears as a focal lesion at earlier ages (approximately 2 wk of age) and usually it evolves into a chronic and diffuse fibrotic injury in late stages of life (42–49 D of age) (Sihvo et al., 2018). The same authors also reported that diminution of blood supply in pectoral muscle tissue occurs in the early stages of WB, which may be associated with the ultrastructural changes of osmotic imbalance as a result of hypoxia and myodegeneration. This evidence suggests that if the major pectoral muscle is under hypoxia at any time during the lifetime of a bird, it might already have developed necrotic tissue and therefore be less prone to the effects of hypoxia compared with WS muscle. Hypoxia results in a reduction of blood vessel density and consequently compromises the blood flow and oxygen supply to the muscle, resulting in an accumulation of metabolites with osmotic properties such as taurine and alanine (Velleman and Clark, 2015), which in our study was confirmed by greater taurine concentrations in WS than that in WB. Another possible reason for the greater amount of taurine in WS breasts might be owing to this compound being produced in tissues exposed to elevated levels of oxidants (Abasht et al., 2016). Xing et al. (2020) reported that modification of calcium homeostasis has been closely associated with an alteration in muscle taurine content, and it has already been reported that high accumulation of intracellular calcium could be one factor that contributes to metabolic changes in myopathic breast (Petracci et al., 2015; Soglia et al., 2019a). It has been suggested that taurine has efficient antioxidant properties, providing protective effects against neurological diseases, and also reduces apoptosis. Li et al. (2017) reported that a high taurine content in liver tissue could play an important role in restoring phospholipid membranes injured by reactive oxygen species, demonstrating a self-repair capacity. Therefore, the increase of taurine levels in WS-affected broilers may be also indicative of a self-protection mechanism aimed at reducing cellular damage caused by exposure to high levels of oxidants.

Other authors also found that taurine is correlated with the occurrence of breast abnormalities in modern commercial broiler breeds (Boerboom et al., 2018; Petracci et al., 2019). The taurine and hypotaurine metabolism pathway was found to be relevant for differentiating WS from WB in this study, especially because of greater amounts of taurine in WS muscle. In addition, the greater relative amounts of some amino acids (such as glutamate, leucine, and serine) and 3-methylhistidine in WS than those in WB suggest greater protein degradation in WS breasts, as 3-methylhistidine is a biomarker for muscle breakdown (Castro Bulle et al., 2007). These changes may also indicate that animals with WS exhibit greater oxidative stress than those with WB, as oxidative stress can influence protein metabolism by decreasing protein synthesis and increasing catabolic rates (Lin et al., 2006).

In contrast, the greater amounts of choline and niacinamide in WB than in WS (Figure 2A) may be a result of differences in fatty acid deposition and collagen

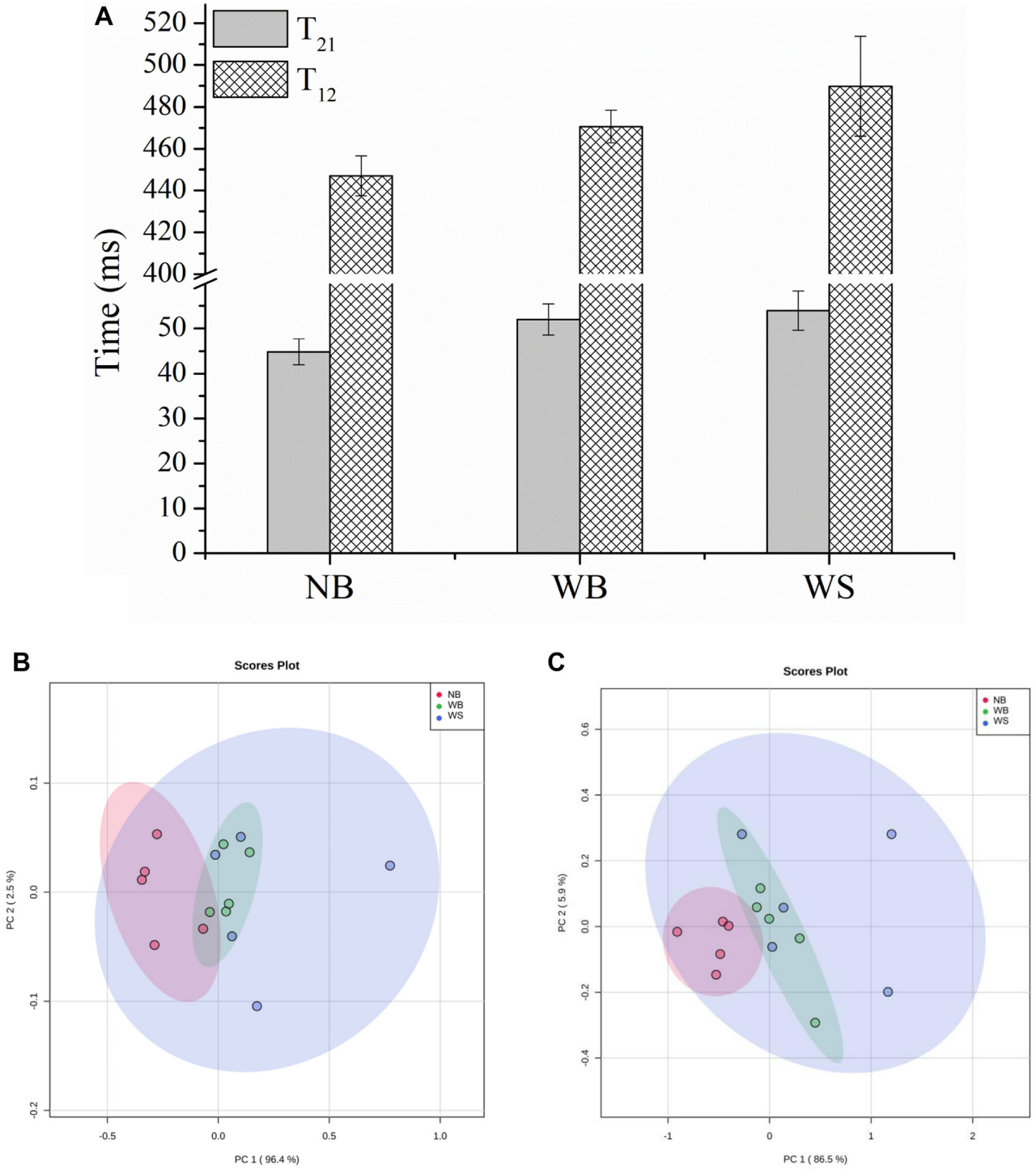

Figure 4. PCA scores plot of relaxometry data: (A) T_{12} and T_{22} values (ms) of the strongest signal calculated by the inverse Laplace transform (ILT) of the CWFP-T_1 and CPMG signals of NB, WS, and WB samples; (B) CPMG pulse sequence; (C) CWFP-T_1 pulse sequence. Abbreviations: CPMG, Carr–Purcell–Meiboom–Gill; CWFP-T_1, continuous wave free precession with a low flip angle; NB, normal breast; WB, wooden breast; WS, white stripping.

metabolism between the 2 pathologies. Microscopically, WB shows inflammation of veins and perivenous lipid deposition and further intense myofiber degeneration, which can be replaced by fibrotic and adipose tissues (Sihvo et al., 2013; Abasht et al., 2019). Choline is correlated with lipid metabolism, and a greater concentration of this metabolite in WB may result in greater lipid deposition and myodegeneration than in WS. In this context, the glycine, serine, and threonine metabolism pathway is relevant for distinguishing WB from WS, owing to the greater amounts of choline and pyruvate in WB than in WS animals (Table 1). Some authors have suggested that animals with WB show changes in lipid metabolism, with higher expression of genes involved in fatty acid uptake (Papah et al., 2018), oxidation (Zambonelli et al., 2016), and degradation of

triglyceride and phospholipids (Mutryn et al., 2015). In the same way, niacinamide is correlated with collagen production (Velleman and Clark, 2015). And, the greater amounts of choline and niacinamide in the WB group, than in the WS group, could suggest that the WB event is characterized by changes in fat metabolism and increased collagen content compared with WS.

Comparison of metabolite profiles of either of the 2 myopathies (WS or WB) with NB confirms the aforementioned findings that WS and WB are indeed different but that they also share some commonalities (Figures 2B, 2C). In terms of similarities, both WS and WB contained lower concentrations of malonate (0.47 and 0.58 mg/g of meat, respectively) than NB (0.79 mg/g of meat) (Figures 2B, 2C). The lower amount of malonate observed in WS and WB breasts may be due to its complexation with SD and hypoxia events in breasts affected by myopathies compared with NB, as explained previously, which confirms data from other studies (Boerboom et al., 2018; Abasht et al., 2019). The lowest concentration of malonate was found in WS breasts, which may indicate that WS presents a more severe hypoxic state than WB. This hypothesis is further supported by a higher concentration of glucose and lower concentration of succinate in WB compared with NB (Figure 2C), which suggests lower glycolytic capacity in WB and decreased Krebs cycle activity in WB breasts. Wooden breast has previously been correlated with lower expression of genes and proteins involved in glycolysis (Mutryn et al., 2015; Kuttappan et al., 2017), decreasing the glycolytic capacity and mitochondrial function (Abasht et al., 2019). This disorder can lead to compromised blood supply and hypoxia in breast tissue, causing defects in ATP synthesis in muscle. The present study found lower amounts of hypoxanthine (in WS than that in NB) and IMP (in both WS and WB than that in NB), suggesting lower blood perfusion for breasts affected by myopathies, oxygen supply, and ATP production in the muscle tissue, with the degradation of ATP resulting in the generation of hypoxanthine via IMP (Muroya et al., 2014).

In addition, both WS and WB contained lower amounts of arginine than NB. Arginine is related to blood supply in tissue and the occurrence of hypoxia, plays an important role in nitric oxide synthesis, and is a potent vasodilator that can enhance blood flow through animal tissues (Khajali et al., 2014). In the present study, it was noted that arginine and proline metabolism is a pathway relevant to the differentiation between NB and either WB or WS. Recently, Boerboom et al. (2018) concluded that the occurrence of myopathies in broilers is linked to vasoconstrictor events that decrease blood flow in tissue and that arginine conversion into citrulline is one of the most impaired metabolic pathways in breasts with severe myopathy.

White-striped breasts also contained greater amounts of taurine than NB (2.67 and 0.79 mg/g of meat, respectively). Pathway analysis confirmed that taurine and hypotaurine metabolism is indeed an important pathway for differentiation of WS and NB groups (Figure 3B). As previously described, the differences in taurine concentrations could be a result of differences in hypoxic state in which taurine accumulation increases in WS breast tissue compared with NB. The greater relative amounts of some amino acids (such as threonine, serine, leucine, glutamine, and aspartate in WS compared with NB and threonine in WB compared with NB; Figures 2B, 2C) and 3-methylhistidine, in WB and WS compared with NB, suggest greater protein degradation in affected breasts, which in turn can be correlated to the greater oxidative stress in broilers that present the myopathies, decreasing protein synthesis and increasing catabolic rates (Lin et al., 2006).

The most important metabolites to differentiate WB from NB were niacinamide and choline (Figure 2C). As described earlier, the former is correlated with greater collagen production and deposition in fibrotic areas, leading to the visible pale appearance and hard consistency of the pectoralis major muscle in WB-affected broilers (Velleman and Clark, 2015). Owing to differences in the levels of niacinamide between NB and WB (Figure 2C), nicotinate and nicotinamide metabolism is the most relevant pathway to differentiate NB from WB (Figure 2C and Table 1). Choline is associated with lipid deposition (as described previously) and myodegeneration (Yang et al., 2018) in WB compared with NB. As consequence, in this study, metabolic pathways related to fat metabolism, such as the glycerophospholipid pathway, glycine, serine, and threonine metabolism, and β-alanine metabolism, are relevant for explaining the differences between NB and WB (Figure 3C).

Conversely to high-resolution ^{1}H-NMR, TD-NMR relaxometry analysis is noninvasive, can be performed on intact and packaged food samples (Flores et al., 2016; Moreira et al., 2016; Bizzani et al., 2017), and is a fast (20 s/sample) and objective method with high predictability (Santos et al., 2014). In this study, chicken breasts were analyzed with the CPMG and CWFP-T_1 pulse sequences, which resulted in multiexponential signals governed by the T_2 and T_1 relaxations times, respectively. Both relaxation times have a strong dependence on the water environment (mobility and water interaction with macromolecules) (Bertram et al., 2007; Tasoniero et al., 2017).

The longer T_{12} and T_{21} values measured in WB and WS than in NB samples indicate greater water mobility in affected breasts. These results agree with the lower water-holding capacity (less bound water) observed in breasts with these myopathies (Zotte et al., 2017). The longer T_{21} values for WB samples also agree with relaxation data published by Tasoniero et al. (2017) and Xing et al. (2017). The longer relaxation times observed in WB and WS breasts are probably due to the greater proteolysis observed in breasts with myopathies, which will increase water mobility owing to the reduction of water–protein interactions (Bertram et al., 2007). As per the relaxation (Supplementary Figures 2A, 2B) and PCA data (Figures 4B, 4C), WS samples showed more variation in terms of the relaxation data than NB and WB.

Data from this pilot study will help to establish reference standards for future metabolic association with broiler breast myopathies. This study not only confirms previous research that metabolomics has the potential to discriminate chicken breast tissue with myopathies from normal chicken breasts but also suggests a way of discriminating between WS and WB. Both WS breasts and WB appear to be correlated with hypoxic conditions, oxidative stress, and collagen metabolism, which confirms previous reports in the literature. However, WB can be differentiated from WS by greater fat and collagen metabolism, and WS presents some metabolites correlated with hypoxia and oxidative stress. Time-domain NMR measurements showed that the occurrence of WS and WB also affects breast water mobilization. Hence, both NMR approaches seem to have potential for detecting myopathies in chicken breasts: Proton NMR metabolomics is for distinguishing between WB and WS and NMR relaxometry as a fast, simple, and noninvasive method to discriminate NB from WB, WS, or both in the package. However, the potential of NMR to correctly differentiate samples still needs to be quantified with a larger number of chicken breasts and robust discrimination equations with their corresponding performance parameters. This study shows that exploring this potential is worth pursuing.

ACKNOWLEDGMENTS

The authors thank São Paulo Research Foundation (FAPESP) for the financial support, grant: 2018/09800-3 and 2019/13656-8.

Conflict of Interest Statement: The authors declare that they have no known competing financial interests or personal relationships that could have appeared to influence the work reported in this paper.

SUPPLEMENTARY DATA

Supplementary data associated with this article can be found in the online version at https://doi.org/10.1016/j.psj.2020.06.066.

REFERENCES

Abasht, B., M. F. Mutryn, R. D. Michalek, and W. R. Lee. 2016. Oxidative stress and metabolic perturbations in wooden breast disorder in chickens. PLoS One 11:1–16.

Abasht, B., N. Zhou, W. R. Lee, Z. Zhuo, and E. Peripolli. 2019. The metabolic characteristics of susceptibility to wooden breast disease in chickens with high feed efficiency. Poult. Sci. 98:3246–3256.

Alnahhas, N., C. Berri, M. Chabault, P. Chartrin, M. Boulay, M. C. Bourin, and E. Le Bihan-duval. 2016. Genetic parameters of white striping in relation to body weight, carcass composition, and meat quality traits in two broiler lines divergently selected for the ultimate pH of the pectoralis major muscle. BMC Genet. 17:61.

Baldi, G., C.-N. Yen, M. R. Daughtry, J. Bodmer, B. Bowker, H. Zhuang, M. Petracci, and D. E. Gerrard. 2020. Exploring the factors contributing to the high ultimate pH of broiler Pectoralis major muscles affected by wooden breast condition. Front. Physiol. 11:343.

Beckonert, O., H. C. Keun, T. M. D. Ebbels, J. Bundy, E. Holmes, and J. C. Lindon. 2007. Metabolic profiling, metabolomic and metabonomic procedures for NMR spectroscopy of urine, plasma, serum and tissue extracts. Nat. Protoc. 2:2692–2703.

Bertram, H. C., I. K. Straadt, J. A. Jensen, and M. Dall Aaslyng. 2007. Relationship between water mobility and distribution and sensory attributes in pork slaughtered at an age between 90 and 180 days. Meat Sci. 77:190–195.

Bizzani, M., D. W. M. Flores, L. A. Colnago, and M. D. Ferreira. 2017. Non-invasive spectroscopic methods to estimate orange firmness, peel thickness, and total pectin content. Microchem. J. 133:168–174.

Boerboom, G., T. Van Kempen, A. Navarro-villa, and A. P. Bonilla. 2018. Unraveling the cause of white striping in broilers using metabolomics. Poult. Sci. 97:3977–3986.

Carrillo, J. A., Y. He, Y. Li, J. Liu, R. A. Erdman, T. S. Sonstegard, and J. Song. 2016. Integrated metabolomic and transcriptome analyses reveal finishing forage affects metabolic pathways related to beef quality and animal welfare. Sci. Rep. 6:1–16.

Castro Bulle, F. C. P., P. V. Paulino, A. C. Sanches, and R. D. Sainz. 2007. Growth, carcass quality, and protein and energy metabolism in beef cattle with different growth potentials and residual feed intakes. J. Anim. Sci. 85:928–936.

Cônsolo, N. R. B., J. Silva, V. L. M. Buarque, A. Higuera-padilla, L. C. G. S. Barbosa, A. Zawadzki, L. A. Colnago, A. Saran Netto, D. E. Gerrard, and S. L. Silva. 2020. Selection for growth and precocity alters muscle metabolism in Nellore cattle. Metabolites 58:1–12.

De Andrade, F. D., A. M. Netto, and L. A. Colnago. 2011. Qualitative analysis by online nuclear magnetic resonance using Carr-Purcell-Meiboom-Gill sequence with low refocusing flip angles. Talanta 84:84–88.

Dransfield, E., and A. A. Sosnicki. 1999. Relationship between muscle growth and poultry meat quality. Poult. Sci. 78:743–746.

Flores, D. W. M., L. A. Colnago, M. D. Ferreira, and M. H. F. Spoto. 2016. Prediction of orange juice sensorial attributes from intact fruits by TD-NMR. Microchem. J. 128:113–117.

Havenstein, G. B. 2006. Performance changes in poultry and livestock following 50 years of genetic selection, 4:30–37.

Khajali, F., M. H. Moghaddam, and H. Hassanpour. 2014. An L-arginine supplement improves broiler hypertensive response and gut function in broiler chickens reared at high altitude. Int. J. Biometeorol. 58:1175–1179.

Kim, Y. S. 2002. Malonate metabolism: biochemistry, molecular biology, physiology and industrial application. J. Biochem. Mol. Biol. 35:443–451.

Kuttappan, V. A., W. Bottje, R. Ramnathan, S. D. Hartson, C. N. Coon, B. W. Kong, C. M. Owens, M. Vazquez-A Non, and B. M. Hargis. 2017. Proteomic analysis reveals changes in carbohydrate and protein metabolism associated with broiler breast myopathy. Poult. Sci. 96:2992–2999.

Kuttappan, V. A., V. B. Brewer, A. Mauromoustakos, S. R. McKee, J. L. Emmert, J. F. Meullenet, and C. M. Owens. 2013. Estimation of factors associated with the occurrence of white striping in broiler breast fillets. Poult. Sci. 92:811–819.

Kuttappan, V. A., Y. S. Lee, G. F. Erf, J. C. Meullenet, S. R. Mckee, and C. M. Owens. 2012. Consumer acceptance of visual appearance of broiler breast meat with varying degrees of white striping. Poutry Sci. 91:1240–1247.

Li, M. H., L. Y. Ruan, J. W. Zhou, Y. H. Fu, L. Jiang, H. Zhao, and J. S. Wang. 2017. Metabolic profiling of goldfish (Carassius auratis) after long-term glyphosate-based herbicide exposure. Aquat. Toxicol. 188:159–169.

Lin, H., E. Decuypere, and J. Buyse. 2006. Acute heat stress induces oxidative stress in broiler chickens. Comp. Biochem. Physiol. A Mol. Integr. Physiol. 144:11–17.

López, K. P., M. W. Schilling, and A. Corzo. 2011. Broiler genetic strain and sex effects on meat characteristics. Poult. Sci. 90:1105–1111.

Moraes, T. B., T. Monaretto, and L. Colnago. 2019. Applications of continuous wave free precession sequences in low-field, time-domain NMR. Appl. Sci. 9:1312.

Moreira, L. F. P. P., A. C. Ferrari, T. B. Moraes, R. A. Reis, L. A. Colnago, and F. M. V. Pereira. 2016. Prediction of beef color using time-domain nuclear magnetic resonance (TD-NMR) relaxometry data and multivariate analyses. Magn. Reson. Chem. 54:800–804.

Mudalal, S., E. Babini, C. Cavani, and M. Petracci. 2014. Quantity and functionality of protein fractions in chicken breast fillets affected by white striping. Poult. Sci. 93:2108–2116.

Mudalal, S., M. Lorenzi, F. Soglia, C. Cavani, and M. Petracci. 2015. Implications of white striping and wooden breast abnormalities on quality traits of raw and marinated chicken meat. Animal 94:728–734.

Muroya, S., M. Oe, I. Nakajima, K. Ojima, and K. Chikuni. 2014. CE-TOF MS-based metabolomic profiling revealed characteristic metabolic pathways in postmortem porcine fast and slow type muscles. Meat Sci. 98:726–735.

Mutryn, M. F., E. M. Brannick, W. Fu, W. R. Lee, and B. Abasht. 2015. Characterization of a novel chicken muscle disorder through differential gene expression and pathway analysis using RNA-sequencing. BMC Genomics 16:399.

Papah, M. B., E. M. Brannick, C. J. Schmidt, and B. Abasht. 2018. Gene expression profiling of the early pathogenesis of wooden breast disease in commercial broiler chickens using RNA-sequencing. PLoS One 13:1–25.

Pereira, F. M. V., S. B. Pflanzer, T. Gomig, C. L. Gomes, P. E. de Felício, and L. A. Colnago. 2013. Fast determination of beef quality parameters with time-domain nuclear magnetic resonance spectroscopy and chemometrics. Talanta 108:88–91.

Petracci, M., S. Mudalal, A. Bonfiglio, and C. Cavani. 2013. Occurrence of white striping under commercial conditions and its impact on breast meat quality in broiler chickens. Poult. Sci. 92:1670–1675.

Petracci, M., S. Mudalal, F. Soglia, and C. Cavani. 2015. Meat quality in fast-growing broiler chickens. Worlds Poult. Sci. J. 71:363–374.

Petracci, M., F. Soglia, M. Madruga, L. Carvalho, E. Ida, and M. Estévez. 2019. Wooden-breast, white striping, and spaghetti meat: causes, consequences and consumer perception of emerging broiler meat abnormalities. Compr. Rev. Food Sci. Food Saf. 18:565–583.

Santos, P. M., C. C. Corrêa, L. A. Forato, R. R. Tullio, G. M. Cruz, and L. A. Colnago. 2014. A fast and non-destructive method to discriminate beef samples using TD-NMR. Food Control 38:204–208.

Savenije, B., E. Lambooij, M. A. Gerritzen, K. Venema, and J. Korf. 2002. Effects of feed deprivation and transport on preslaughter blood metabolites, early postmortem muscle metabolites, and meat quality. Poult. Sci. 81:699–708.

Sihvo, H. K., N. Airas, J. Lindén, and E. Puolanne. 2018. Pectoral vessel density and early ultrastructural changes in broiler chicken wooden breast myopathy. J. Comp. Pathol. 161:1–10.

Sihvo, H., K. Immonen, and E. Puolanne. 2013. Myodegeneration with fibrosis and regeneration in the pectoralis major muscle of broilers. Vet. Pathol. 51:619–623.

Soglia, F., M. Mazzoni, and M. Petracci. 2019a. Spotlight on avian pathology: current growth-related breast meat abnormalities in broilers. Avian Pathol. 48:1–3.

Soglia, F., A. K. Silva, L. M. Lião, L. Laghi, and M. Petracci. 2019b. Effect of broiler breast abnormality and freezing on meat quality and metabolites assessed by 1 H-NMR spectroscopy. Poult. Sci. 98:7139–7150.

Tasoniero, G., H. C. Bertram, J. F. Young, A. Dalle Zotte, and E. Puolanne. 2017. Relationship between hardness and myowater properties in wooden breast affected chicken meat: a nuclear magnetic resonance study. LWT 86:20–24.

Trocino, A., A. Piccirillo, M. Birolo, G. Radaelli, D. Bertotto, E. Filiou, and M. Petracci. 2015. Effect of genotype, gender and feed restriction on growth, meat quality and the occurrence of white striping and wooden breast in broiler chickens. Poult. Sci. 94:2996–3004.

Velleman, S. G., and D. L. Clark. 2015. Histopathologic and myogenic gene expression changes associated with wooden breast in broiler breast muscles. Avian Dis. 59:410–418.

Venkataramanan, L., Y. Q. Song, and M. D. Hürlimann. 2002. Solving Fredholm integrals of the first kind with tensor product structure in 2 and 2.5 dimensions. IEEE Trans. Signal Process. 50:1017–1026.

Wold, J. P., I. Mage, A. Løvland, K. W. Sanden, and R. Ofstad. 2019. Near-infrared spectroscopy detects woody breast syndrome in chicken fillets by the markers protein content and degree of water binding. Poult. Sci. 98:480–490.

Wold, J. P., E. Veiseth-Kent, V. Høst, and A. Løvland. 2017. Rapid on-line detection and grading of wooden breast myopathy in chicken fillets by near-infrared spectroscopy. PLoS One 12:1–16.

Xing, T., X. Zhao, M. Han, L. Cai, S. Deng, G. Zhou, and X. Xu. 2017. A comparative study of functional properties of normal and wooden breast broiler chicken meat with NaCl addition. Poult. Sci. 96:3473–3481.

Xing, T., X. Zhao, X. Xu, J. Li, L. Zhang, and F. Gao. 2020. Physiochemical properties, protein and metabolite profiles of muscle exudate of chicken meat affected by wooden breast myopathy. Food Chem. 316:126271.

Yang, X., F. Yin, Y. Yang, D. Lepp, H. Yu, Z. Ruan, C. Yang, Y. Yin, Y. Hou, S. Leeson, and J. Gong. 2018. Dietary butyrate glycerides modulate intestinal microbiota composition and serum metabolites in broilers. Sci. Rep. 8:1–12.

Zambonelli, P., M. Zappaterra, F. Soglia, M. Petracci, F. Sirri, C. Cavani, and R. Davoli. 2016. Detection of differentially expressed genes in broiler pectoralis major muscle affected by white striping – wooden breast myopathies. Poult. Sci. 95:2771–2785.

Zawadzki, A., L. O. R. Arrivetti, M. P. Vidal, J. R. Catai, R. T. Nassu, R. R. Tullio, A. Berndt, C. R. Oliveira, A. G. Ferreira, L. F. Neves-Junior, L. A. Colnago, L. H. Skibsted, and D. R. Cardoso. 2017. Mate extract as feed additive for improvement of beef quality. Food Res. Int. 99:336–347.

Zotte, A. D., G. Tasoniero, E. Puolanne, H. Remignon, M. Cecchinato, E. Catelli, and M. Cullere. 2017. Effect of "wooden breast" appearance on poultry meat quality, histological traits, and lesions characterization. Czech J. Anim. Sci. 62:51–57.